

https://dspace.org/

Removal of Nickel from Nickel SulfiteFire Assay Dissolution Filtrate Through Precipitation

Mothepane Mabowa; A Mkhohlakali; SAM Mokoena; James Tshilongo; Luke Chimuka

https://hdl.handle.net/10539/43107
WOS

Downloaded from a DSpace repository. https://dspace.org/

ACS OMEGA

Open Access

This article is licensed under CC-BY-NC-ND 4.0

http://pubs.acs.org/journal/acsodf

Article

Removal of Nickel from Nickel Sulfite-Fire Assay Dissolution Filtrate Through Precipitation

Happy Mothepane Mabowa,* Andile Mkhohlakali, Sam Mokoena, James Tshilongo, and Luke Chimuka

Cite This: *ACS Omega* 2024, 9, 5592−5600

Read Online

ACCESS | Metrics & More | Article Recommendations | Supporting Information

ABSTRACT: This study responds to stringent environmental regulations and increasing focus on resource conservation by exploring economically viable refining technologies through recycling. With the rising costs of filtrate disposal, there is a significant emphasis on removing and recycling valuable constituents, particularly nickel and copper (Ni and Cu). Herein, we employ analytical techniques with the aim of investigating an alternative method for recovering Ni and other valuable metals from a nickel sulfide-fire assay filtrate using *S*-curve precipitation under optimal conditions. The waste from the fire assay procedure contains substantial amounts of Ni and other critical metals, with concentrations of 62.7 g/L of Ni and 3.87 g/L of Cu. Prior to precipitation, traditional solvent extraction was used for Cu extraction, selectively removed before separating primary impurities such as iron (Fe). A pivotal aspect of this research involves applying *S*-curve precipitation with precise parameters at different pH levels. Analytical techniques reveal a minor depletion occurs as Ni is separated from Fe at a pH of 2.5, resulting in the formation of a refined Ni stream that is then refined into a mixed hydroxide $Ni(OH)_2$ product. The efficiency of 5,8-diethyl-7-hydroxydodecan-6-oxime (LIX 63−70) in extracting value-added metals from fire assay waste is exceptionally high, integrating recycling and repurposing of value-added base metals to promote a circular economy.

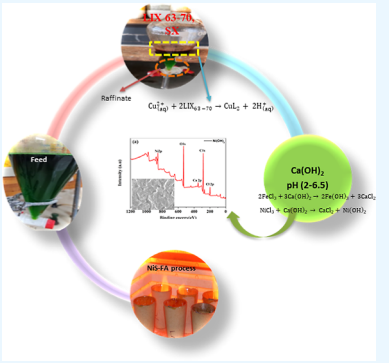

Downloaded via UNIV OF THE WITWATERSRAND on November 7, 2024 at 12:51:55 (UTC).
See https://pubs.acs.org/sharingguidelines for options on how to legitimately share published articles.

1. INTRODUCTION

Nickel (Ni) is a vital metallic element widely utilized in numerous industries due to its outstanding corrosion resistance. Estimated to be present in the Earth's crust in a concentration of 80 ppm, Ni is a silver-white, hard, and ductile metal that ranks 24th in abundance.[1] Ni byproducts, like those from spent batteries, present health and environmental risks through air, water, and soil pathways. Mitigation requires strict regulations, advanced recycling, and comprehensive treatment. Ongoing research and public awareness are vital for addressing challenges posed by Ni pollutants.[2,3] Exposure to surroundings with high levels of Ni pollution can cause a range of pathological effects in people, including contact dermatitis, lung fibrosis, kidney, and cardiovascular disorders. In addition to Ni being economically valuable, the Ni price flaunting is similar to other metals, and the price is relatively high. There have been various techniques reported in previous studies for the removal of Ni from different types of waste. Two different approaches can be applied to solid wastes: (i) hydrometallurgy, a method that involves solvent extraction (SX), leaching waste metal into a solution and recovering the target metal; (ii) pyrometallurgy, this method involves treating waste metal with heat to recover the target metal.[4,5] Herein, we address the environmental and economic aspects of Ni removal from nickel sulfide (NiS) collection from the novel fire assay fusion for precious group element (PGE) filtrate dissolution waste. NiS is a widely used method to collect PGEs.[6] Ni recycling has attracted considerable interest to provide options for reuse and repurposing the value-added metal at the same time circumventing the environmental pollution risk.[1] The method involves fusing Ni, sulfur, sodium carbonate, borax, and a PGE-containing sample in a clay crucible at 1000−1300 °C. The resulting NiS button is crushed, dissolved in hydrochloric acid (HCl), and filtered to obtain a precious metal residue, including PGEs. This process is commonly used in analytical chemistry for isolating and concentrating trace elements and precious metals from samples. The filtrate containing high concentrations of Ni and other valuable metals is disposed of as process waste. The waste contains Ni and a variety of metal contaminants, including copper, iron, zinc, sodium, potassium, lead, cobalt, aluminum, manganese, silica, chrome, and magnesium (Cu, Fe, Zn, Na, K, Pb, Co, Al, Mn, Si, Cr, and Mg). Copper and nickel in waste are valuable elements that can be further processed and purified.

Methods like chemical precipitation, electrolytic membranes, and ion exchange are utilized to eliminate impurity metal ions and refine Ni aqueous solutions.[7,8] Despite their effectiveness, these techniques face limited adoption due to their high

Received: October 3, 2023
Revised: December 26, 2023
Accepted: December 28, 2023
Published: January 25, 2024



© 2024 The Authors. Published by American Chemical Society

expenses, impracticality for small-scale use, and challenges associated with material regeneration.[9] Among these approaches, precipitation is the most commonly employed method for waste treatment, favored for its cost-effectiveness and suitability for large-scale applications. However, traditional precipitation methods, which involve lime, sulfides, or hydroxides, generate a voluminous sludge that cannot be reused and requires disposal in landfills. This not only poses environmental hazards but also results in the loss of valuable minerals. Additionally, subsequent treatment incurs significant operational costs, especially in terms of energy consumption.[10]

Several treatment processes have been reported in the literature for the Ni-ion mitigation from liquid waste, including adsorption,[11] ion exchange,[12] chemical precipitation,[13] and electrochemical methods: electrode ionization.[14] Hydroxide precipitation, a conventional method for metal plating waste treatment, relies on the low solubility of metal hydroxides under alkaline conditions. This process involves forming metal hydroxide solid phases that are then separated from wastewater through sedimentation, flotation, and filtration. The sulfide is another procedure that results in minimal solubility of metal sulfides, proving efficient for both free and complex metals. This method is efficient in free and particularly complex metals.[15] The metal sulfide waste has a strong acid generation potential, which makes it undesirable for disposal. However, the associated metal sulfide waste poses challenges due to its potential for strong acid generation, making disposal undesirable. Coagulants, including ferric chloride ($FeCl_3$), alum, and various polyelectrolytes, are commonly used in hydroxide precipitation applications to address solid formation and separation issues and enhance the clarity of the supernatant.

Concentrated nickel hydroxide $Ni(OH)_2$ or sulfides in precipitated sludge are extremely hazardous and life-threatening wastes that must be disposed of at a high cost to the industry using specialized facilities.[3] It is essential for environmental preservation and resource conservation that Ni-containing wastewater is effectively recovered and reused. The development of closed-recycle systems or effluent-free technology is critical. Analyzing trace elements in wastewater involves employing diverse inorganic techniques.[16−18] To the best of our knowledge, there is no $Ni(OH)_2/NiSO_4$ recovered from fire essay waste reported in the literature. Herein, we aim to remove and recover nickel from the nickel sulfide fire assay dissolution filtrate through SX and precipitation from the PGE filtration solution (waste).

2. RESULTS AND DISCUSSION

2.1. Head Sample Filtrate Solution Waste. The major metals in the filtrate solution were Ni (62.7 g/L), Fe (4.72 g/L), and Cu (3.87 g/L). There were also notable concentrations of Zn, Na, K, Pb, Co, Al, Mn, Si, Cr, and Mn. Although the solution was predominantly chloride media, there was a notable concentration of sulfur, which suggests some metals were associated with sulfur. From the literature survey, it has been observed that no viable processes are reported to recover Cu and Ni from filtrate solution from PGE's preparation. Based on the concentration of the major elements, Ni and Cu are commonly regarded as valuable metals, while Fe is classified as impurity elements. Furthermore, the concentration levels of both Ni and Cu are sufficiently high and justify any effort for recovery. Contrary, the concentration of all of the elements listed under minor elements is too low to be considered for recovery.

Table 1 presents the chemical analyses of the head sample. The results show that the feed solution contained 280 g/L hydrochloric acid (HCl) and a chlorine (Cl) concentration of 80 g/L. This confirms that the solution was prepared by dissolving the solid material in concentrated HCl (32%) and that the solution is in a chloride matrix. The presence of HCl and varying Ni concentrations affects ion peak intensities in the analysis of high-purity Ni samples using inductively coupled plasma mass spectroscopy (ICP−MS). Existing literature suggests that the influence of chlorine (Cl) on the matrix is insignificant.[18] Nevertheless, when dealing with Ni samples with a high content, the matrix effects were observed to inhibit the signals of the analyte isotopes. The major metals in the filtrate solution were Ni (62.7 g/L), Fe (4.72 g/L), and Cu (3.87 g/L). There were also notable concentrations of Zn, Na, K, Pb, Co, Al, Mn, Si, Cr, and Mn. Although the solution was predominantly chloride media, there was a notable concentration of sulfur, which suggests some metals were associated with sulfur. From the literature survey, it has been observed that no viable processes are reported to recover Cu and Ni from the filtrate solution from PGE's preparation.

Table 1. Chemical Composition of the Feed Solution

element	feed	raffinate	major elements
	concentration (g/L)		
Ni	62.7	62.7	
Fe	4.72	2.6	
Cu	3.87	0.8	
Cl	80	80	
HCl	280	280	
	concentration (ppm)		minor elements
Zn	73.9	71.6	
K	22.5	22.5	
Na	210	22.5	
Pb	10.2	10.2	
Co	9.8	9.8	
Al	7.3	7.3	
Mn	6.7	0.48	
Ca	4.53		
Si	4.11		
Cr	3.51	3.51	
Mg	2.69		
As	0.26	0.26	
Ag	0.25		
Cd	0.23	0.23	
S	162	144	

Based on the concentration of the major elements, Ni and Cu are commonly regarded as valuable metals while Fe is classified as impurity elements. Furthermore, the concentration levels of both Ni and Cu are sufficiently high and would justify any effort for recovery. Contrary, the concentration of all the elements listed under minor elements is too low to be considered for recovery.

2.2. SX of Copper (Cu). The pre-extraction stage of copper (Cu) before precipitation using 5,8-diethyl-7-hydroxydodecan-6-oxime (LIX 63−70) typically involves the formation of a complex between the oxime groups in the reagent and the Cu ions. The utilization of SX as a pre-extraction method is a strategic measure to prevent Cu loss during precipitation in the

https://doi.org/10.1021/acsomega.3c07623
ACS Omega 2024, 9, 5592−5600

presence of iron (Fe). In tradition, Cu precipitation processes coexistence of Fe leads to coprecipitation, causing Cu loss in the form of Cu−Fe hydroxide precipitates, as illustrated in Figure S1 and Table S1 in the Supporting Information. The detection of Cu in energy-dispersive X-ray spectroscopy (EDX) analysis during the precipitation of Fe_2O_3 in Figure S1 highlights the need to prevent Cu loss. To address this, a pretreatment step employing SX is applied, selectively extracting Cu and enhancing the overall efficiency of copper extraction.

The specific reaction can be represented as indicated

$$Cu^{2+}_{(aq)} + 2LIX_{63-70} \rightarrow CuL_2 + 2H^{+}_{(aq)} \quad (1)$$

where $Cu_{(aq)}^{2+}$ (3.87 g/L) represents Cu ions in the aqueous phase, CuL_2 represents the complex formed with LIX 63−70. Two molecules (denoted by $2LIX_{63-70}$) of the oxime reagent LIX 63−70 and $2H^{+}_{(aq)}$ indicate protons that may be involved in the complex formation process.

In this study, the extraction of Cu using LIX 63−70 was applied, focusing on the initial complex formation between the oxime groups of the reagent and Cu ions. This intricate process led to the efficient transfer of Cu from the pregnant leach solution/aqueous phase to the organic phase, accomplished at ambient temperature and low pH values within a concise 15 min contact time. The oxime functional groups exhibited a notable affinity for metal ions, particularly Cu, contributing to the high extraction efficiency of 97% as described and compared in the literature.[19,20] The resulting aqueous phase, termed the raffinate, revealed a Cu concentration of 800 ppm as determined by inductively coupled plasma−optical emission spectroscopy (ICP−OES). A comparative analysis with Acorga M5640 and Mextral 5640H underscored LIX 63−70s efficacy demonstrating notably faster equilibrium conditions.[21] Furthermore, the previous study highlighted the pH dependency of Cu extraction, emphasizing the influence on Acorga M5640 and Mextral 5640H performance.[20] This research, which reported the extraction of 97% Cu using LIX 63−70 at room temperatures for a contact time of 15 min, provides valuable insights into the effectiveness of the solvent as an extractant for Cu under specific conditions, contributing to the broader understanding of SX processes.[22] The raffinate concentration reacted with lime to produce iron(III) hydroxide $Fe(OH)_3$ precipitate at pH 2.5, as shown in eq 2, were analyzed by ICP−OES, and the results are shown in Table 2. The precipitate cake was dried and characterized by X-ray diffraction (XRD) and scanning electron microscopy (SEM).

Table 2. Lime Consumption Analyses

pH	lime consumption, Ni (kg/kg)	cumulative lime utilization, %
2	2.8	71
2.5	2.83	71
3	2.85	72
3.5	2.9	73
4	2.94	74
4.5	3.02	76
5	3.08	78
5.5	3.33	84
6	3.75	95
6.5	3.87	98
7	3.92	99
7.5	3.96	100

2.3. Precipitation *S*-Curve for Major Elements. The precipitation experiments conducted have elucidated the profound impact of the solution pH and metal concentration on the precipitation kinetics of dissolved ions, particularly in the initial phase of the precipitation process. Figure 1 encapsulates the precipitation *S*-curves delineating the precipitation behaviors of major metals within the raffinate solution. Analysis of the *S*-curve plots reveals a distinctive pH-dependent precipitation hierarchy among Fe, Cu, and Ni.

Notably, the results indicate that Fe precipitates at a lower pH than Cu and Ni. Achieving complete precipitation of Fe was realized at a pH of 2.5 as illustrated in eq 2, underscoring its heightened proclivity for precipitation under mildly acidic conditions. In contrast, Cu demonstrated full precipitation at a marginally higher pH of 4.5, signifying differential pH sensitivity in its precipitation dynamics. Ni exhibited distinct behavior, with complete removal from the solution occurring at a pH of 6.5 as denoted in eq 3, further accentuating its unique precipitation profile compared to both Fe and Cu. These findings contribute a nuanced understanding of the pH-mediated precipitation characteristics of major metals in the raffinate solution, presenting valuable insights for the optimization of the precipitation process in the selective separation and recovery of Fe, Cu, and Ni.

$$2FeCl_3 + 3Ca(OH)_2 \rightarrow 2Fe(OH)_3 + 3CaCl_2 \quad (2)$$

The precipitate cake of $Fe(OH)_3$ was subjected to drying in an oven at a temperature of 52 °C. This drying process is likely employed to remove any remaining moisture content from the precipitate, leading to the formation of a dry and stable product. The temperature is indicative of a relatively mild drying condition, often chosen to prevent excessive heat-induced transformations while efficiently evaporating moisture. This step is crucial in many chemical processes to obtain a solid and dry form of the $Fe(OH)_3$ precipitate for further analysis or for use in subsequent stages of experimentation.

Although both Cu and Ni were removed at relatively higher pH values compared to Fe, the precipitation of these metals was initiated at pH 2 for Ni and pH 2.5 for Cu. This observation suggests that while there is potential for selectively separating Ni and Cu from Fe through precipitation, the process inherently leads to the loss of both metals. According to the results depicted in Figure 1, it can be seen that the optimal separation of Ni and Cu from Fe could be achieved at a pH of 2.5. This would result in losses of 10% for Ni and 8% for Cu. Consequently, the pre-extraction of Cu emerges as a strategically suitable stage to prevent the loss of 8% of Cu during subsequent precipitation processes.

$$NiCl_3 + Ca(OH)_2 \rightarrow CaCl_2 + Ni(OH)_2 \quad (3)$$

The metal concentration profiles in Figure 2 show that there was a significant drop in the concentrations of Ni, Cu, and Fe after neutralization to pH 2.0. The drop in concentration of Cu and Ni was caused by a dilution with the addition of the 20% lime slurry, while the drop in Fe concentration was caused by both precipitation and dilution. The concentration of Fe at pH 2.5 was <2 ppm (parts per million) which correlates with the precipitation *S*-curves which reported complete precipitation of Fe and the precipitation of rust-colored $Fe(OH)_3$. The Cu concentration dropped slightly between pH 2.0 and 3.5, and a significant drop below 2 ppm was achieved at pH 5.5.

The concentration of Cu ions, as well as the surface electrical properties of materials and their interaction with ions,

https://doi.org/10.1021/acsomega.3c07623
ACS Omega 2024, 9, 5592−5600

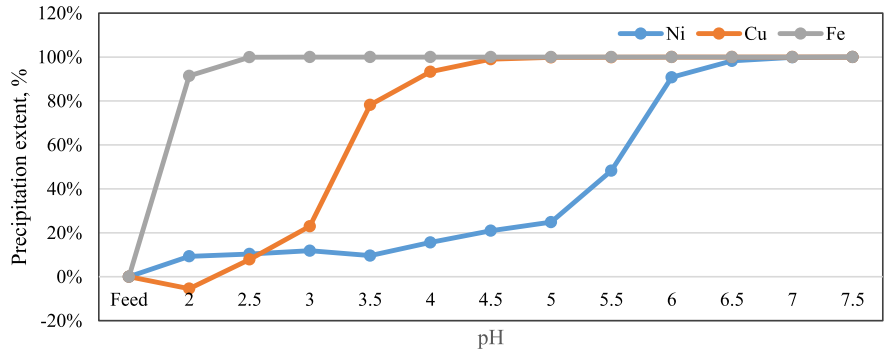

Figure 1. Precipitation *S*-curve plots of major elements (Cu, Fe, and Ni).

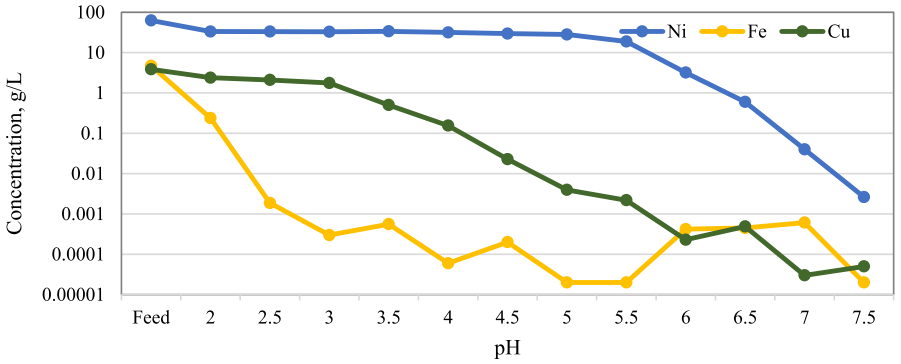

Figure 2. Metal concentration vs pH for major elements (Ni, Cu, and Fe).

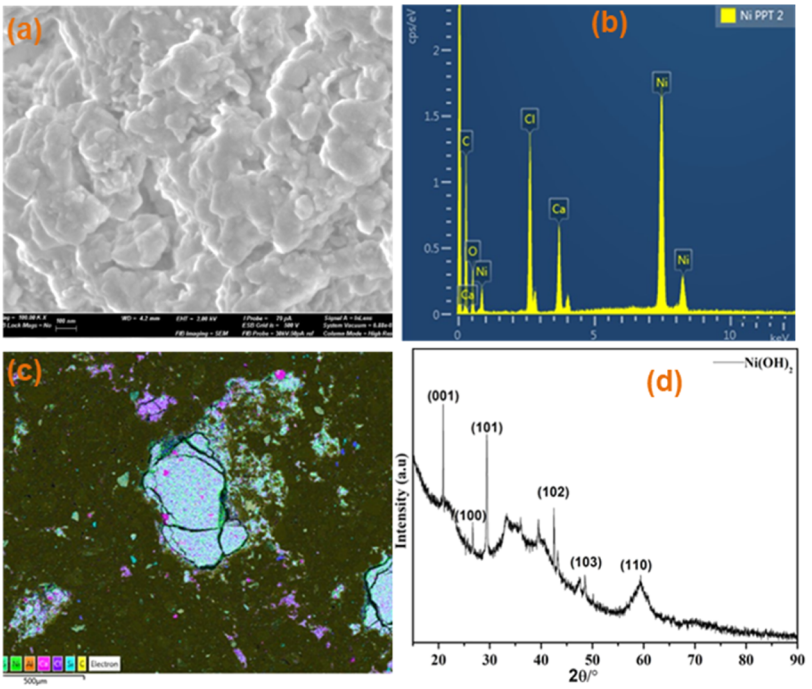

Figure 3. SEM micrograph (a); EDX spectra (b); SEM–EDX overall element distribution map (c); and XRD pattern (d) of $Ni(OH)_2$.

is significantly influenced by the pH of the solution. These observations were made during contact times ranging from 10 to 120 min. The adsorption performance ranged from 50.7 to 93.0% at pH 5.5, with contact periods ranging from 10 to 120 min. This variability is attributed to the enhanced adsorption of Cu at increased pH levels. Despite different efficiency intervals, the efficiency gap remained nearly constant at the same contact time. The research reported that the concentration of Ni was stable at 33 g/L between pH 2.0 and 5.0, and a steep drop was noted between pH 5.0 and 7.5. These results confirm that Fe can be separated from Cu and Ni at pH 2.5 with minimum losses. The absorption of Ni(II) decreases as the solution's pH rises. Initially, the time-growth plots show a curved pattern due to rapid removal, eventually flattening as

https://doi.org/10.1021/acsomega.3c07623
ACS Omega 2024, 9, 5592−5600

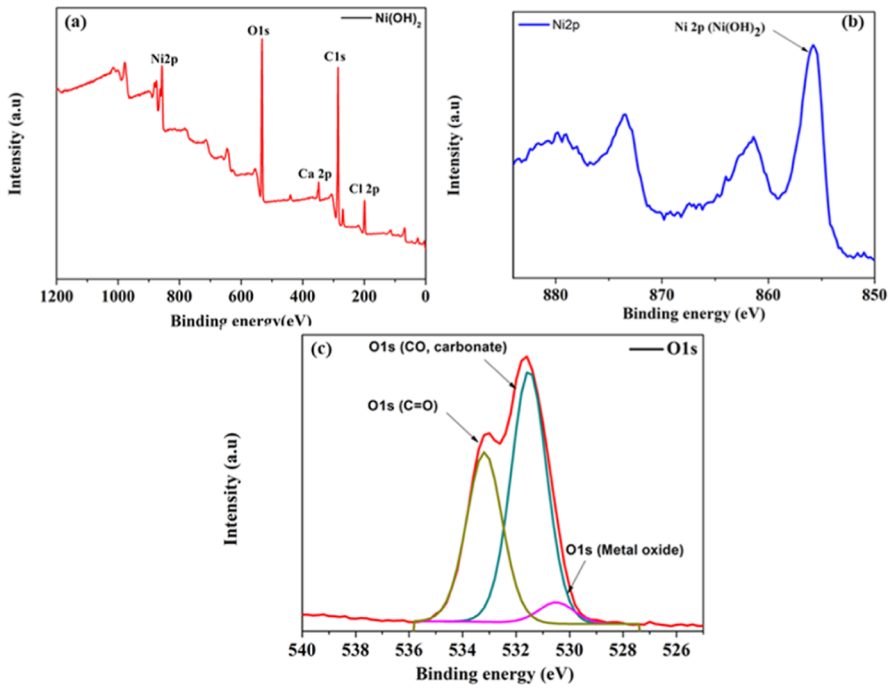

Figure 4. XPS spectra survey of $Ni(OH)_2$ (a); Ni 2p spectra (b); and O 1s spectra of β-$Ni(OH)_2$ (c).

the removal process slows to near saturation. However, the highest adsorption of Ni(II) occurs under alkaline conditions. Figure 2 indicates that Ni(II) uptake is more pronounced at alkaline pH levels up to 5.0, with minimal removal, and it increases progressively with a further increase in pH, reaching its peak at pH 6.5.

Then, generally, there was a decrease in concentrations of heavy metals with an increase in pH. The summarized analyses of lime consumption for the *S*-curve test are provided inTable 2, these was analyzed by ICP−OES and the Na, and K were analyzed by atomic absorption spectroscopy (AAS). It can be noted from the results that a significant portion (71%) of the lime was utilized to neutralize the acid to pH 2.0. Only 7% of the total lime was used to increase the pH from 2.0 to 5.0 and achieve complete Fe and Cu precipitation. The remaining 22% of lime was used as Ni at pH 7.5. The total lime consumption for precipitation *S*-curve was 3.96 kg/kg of available Ni.

2.3.1. Structural and Morphological Properties. The decline in Cu content within the precipitates under elevated acid concentrations, illustrated in Figure 3a, is ascribed to the rise in the equilibrium ferric (Fe^{3+}) concentration in the solution is also depicted in Figure S1 and Table S1. This escalation leads to a slower nucleation rate, resulting in larger particles, as evidenced in Figure 3a, and a comparatively reduced adsorption of divalent ions or solution occlusion. This phenomenon aligns with the findings of Pham et al.,[18] who also noted an enlargement in the particle size under higher acid concentrations showing a flower-like typical $Fe(OH)_3$ hierarchical nanostructure as a result of controlled nucleation.

SEM images in Figure 3a depict the layered granule with nearly spherical particles which is typical $Ni(OH)_2$ and this corroborates with previous literature.[23] The rough surface may correspond to high oxides on the Ni surface, and rough agglomeration also corresponds to typical formation during the precipitation process. In addition, the aggregation may be attributed to nonpost treatment. EDX confirms the existence of Ni and O (of the hydroxide) from the oxides. Interestingly, the EDS spectra show no Cu traces which indicates that Cu was loaded to the organic phase successfully, as displayed in eq 1, before the precipitation process. The Ca impurities may be attributed to Ca from the lime and $CaCl_2$, as illustrated in eq 3. Furthermore, the element map in Figure 3c displays the Ni distribution and other elements corresponding to the EDX spectra. Figure 3b depicts the XRD pattern which represents the β-$Ni(OH)_2$ formed during the precipitation process. The pattern confirms the precipitation of $Ni(OH)_2$, all diffraction peaks indicate the β-$Ni(OH)_2$ hexagonal phase and the peaks indexed 2θ values 24, 29, 30, 45, 50, and 60° corresponding to (001), (100), (101), (102), (103), and (110), respectively,[24,25] and matches with the joint committee on powder diffraction standards(JCPDS):73-1520 standard.

The states of the chemical composition and electronic structure of the $Ni(OH)_2$ surface are characterized by X-ray photoelectron spectroscopy (XPS), as displayed in Figure 4. The spectra survey of $Ni(OH)_2$ from 0 to 1300 eV. The peaks allocated around 860, 510, and 300 eV, are assigned to Ni 2p, O 1s,[26] and C 1s, which indicates that $Ni(OH)_2$ was precipitated successfully at pH 6.5, as supported by Table S1. The results collaborate with the previous studies.[27] The peak photoelectron peaks around 200 and 350 eV are due to Cl and Ca from the HCl (from the waste matrix) impurities and lime, respectively. Figure 4b shows the spectrum of Ni 2p, and the peaks located around 873 and 855.87 eV are ascribed to Ni ($2p_{1/2}$) and Ni ($2p_{3/2}$) respectively. The O 1s photoelectron peak could be deconvoluted into three peaks, as shown in Figure 4c. The hydroxyl species in the $Ni(OH)_2$ surface is confirmed by the O 1s of the metal oxide located around 531 eV. Other O 1s peaks indicate the carbon dioxide (CO_2) impurities observed with Fourier transform infrared (FTIR) in Figure 5.

In Figure 5, the FTIR spectra of $Ni(OH)_2$ are presented, revealing distinctive peaks at 450−600 and 1100 cm^{-1}, corresponding to the ν(Ni−O) stretching vibrations in the β-phase of $Ni(OH)_2$ and ν(O−Ni−O), respectively. Another

https://doi.org/10.1021/acsomega.3c07623
ACS Omega 2024, 9, 5592−5600

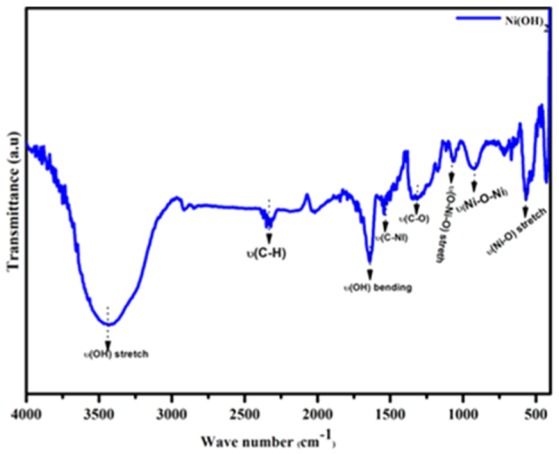

Figure 5. FTIR spectra of $Ni(OH)_2$.

stretching vibration band around 1000 cm^{-1} is associated with ν(Ni−O−Ni). These observations are consistent with the literature.[24] Noteworthy, the strong bending vibration band that can be seen around 1600 cm^{-1} is attributed to a hydroxyl group of $Ni(OH)_2$. The broad stretching vibration peak 3450 cm^{-1} is ascribed asymmetric ν(OH) stretching mode from water/metal hydroxyl in α-phase ν(Ni−OH). The sharp peak around 1620 cm^{-1} is ascribed to δ(OH) bending vibration[28] on the Ni surface. The aforementioned results confirm that $Ni(OH)_2$ was precipitated successfully. The other vibration bands around 2200, and 1330 cm^{-1} are attributed to ν(C−O) stretching and ν(C−H) from the minor impurities. The latter results collaborate with the XPS results in Figure 4, which indicate that Cu was completely loaded in the organic phase, as illustrated in eq 1, and only $Ni(OH)_2$ was precipitated at pH 6.5. All functional groups are summarized in Table 3, and they are consistent with Figure 4. These are also consistent with Tables S2 and S3, which illustrate the XPS and EDX results, which is $Ni(OH)_2$.

Table 3. Summary of FTIR Results Showing the $Ni(OH)_2$ Functional Groups

functional groups	wave number (cm^{-1})	assignment
ν(SiO), ν(O−Ni−O)	470−800	NiO and Ni−OH
ν(OH)	3400	asymmetric stretch vibration of OH of H_2O and β-$Ni(OH)_2$ phase
δ(OH)	1650	bending vibration of OH of H_2O
ν(C−H)	2300	C−H stretching due to C impurities
ν(C−O)	1460	CO stretching vibration, due to carbon/carbonate impurities

Figure 6a,b shows the SEM and EDX of $Ni(OH)_2$ with high Fe impurity at pH 2.5, the surface morphology is similar to SEM micrographs of $Ni(OH)_2$ illustrated in Figure 3a, a rough surface with layered granules and nearly spherical particles; however, the EDX indicates the presence of Fe in $Ni(OH)_2$. These results confirm the expected experimental results according to the *S*-curve where Fe remained in Ni-raffinate at pH 2.5. Noteworthy, the Fe impurity is very high, and the XRD indicates the Fe peaks with the slight 2θ shift around 50 °C; the results corroborate with XPS (Figure 4). The 2θ shift may be attributed to the substitution of Ni atoms in the crystal structure by Fe atoms. The EDX spectra also indicate the high Ca content as an impurity, which is attributed to lime $Ca(OH)_2$ used during the precipitation. The latter results are consistent with XPS results in Tables S3 and S4 of the Supporting Information.

In Figure 7, Fe, Ni, and O were consistently detected in the survey spectra of $Fe_2O_3/Ni(OH)_2$ from 0 to 1000, as displayed in Figure 7a. The photoelectron peaks around 880 and 720 and 520 eV are assigned to Ni 2p and Fe 2p, respectively. The results are consistent with EDX results, which indicate that at pH 2.5, both Fe and Ni precipitated. The peaks allocated around 855 and 875 eV are ascribed to Ni $2p_{3/2}$, and Ni $2p_{1/2}$, respectively. The peaks show the characteristic XPS peaks of Ni. Around 712 and 726 correspond to Fe $2p_{2/3}$ and Fe $2p_{1/2}$, and this method could be attributed to Fe^{3+}. The results show strong agreement with EDX, which shows the existence of Fe, Ni, and $(OH)_2$ species. The existence of Fe and Ni at pH 2.5 is also displayed in the EDX results in Table S1 and the XPS results in Table S4.

3. CONCLUSIONS

Separation of $Ni(OH)_2$ by SX from the fire essay waste was successful; LIX 63−70 exhibit the high efficiency to load Cu in the organic layer and liberate Ni in the aqueous phase. In addition, chemical analyses of the head sample showed that the solution was very acidic with an HCl concentration of 163 g/L and contained high Ni and Cu, with concentrations of 62.7 and 3.87 g/L, respectively. Fe was the only notable impurity element with a concentration of 4.72 g/L. The results for the precipitation *S*-curve showed that Ni and Cu can be separated from Fe at pH 2.5 with minimum losses and produce a Ni−Cu stream that could be processed further to produce a mixed hydroxide product.

The total lime consumption for neutralizing the feed solution to pH 7.5 was 3.96 kg/kg of Ni. About 71% (i.e., 2.80 kg $Ca(OH)_2$/kg Ni) of the total lime consumption was used to neutralize the acid in the solution and obtain pH 2.0. In general, the filtrate solution produced during PGE analyses contains relatively high concentrations of valuable metals. Physico-chemical characterization of the precipitate is in strong agreement with the precipitation *S*-curve. XRD showed a crystalline β-$Ni(OH)_2$ phase similar to FTIR which precipitated at pH 6.5. In addition, the nondetected Cu and Fe at pH 6.5, as confirmed by EDX and XPS indicates that LIX 63−70 loaded the Cu in the organic phase and only $Ni(OH)_2$ precipitated at pH 6.5. Interestingly, EDX and XRD showed the composite of $Fe_2O_3/Ni(OH)_2$ at pH 2.5, which corroborates the precipitation *S*-curve, indicating that traces Ni precipitated with Fe as impurity. The classical solvent separation using LIX 63−70 exhibits high efficiency for separating value-added metal from fire assay waste. The aforementioned approach provides with recycling and repurposing of value-added base metal for the circular economy.

4. MATERIALS AND METHODS

4.1. Material and Reagents. The Ni filtrate used in this study was collected from NiS Laboratory within the Analytical Chemistry Division in Randburg South Africa, 5,8-diethyl-7-hydroxydodecan-6-oxime (LIX 63−70) supplied by BASF South Africa (Pty) Ltd. All reagents were analytical grade without further modification, ACS, ISO grade, sodium hydroxide A.R., 65% (v/v) nitric acid (w/w), and sodium

https://doi.org/10.1021/acsomega.3c07623
ACS Omega 2024, 9, 5592−5600

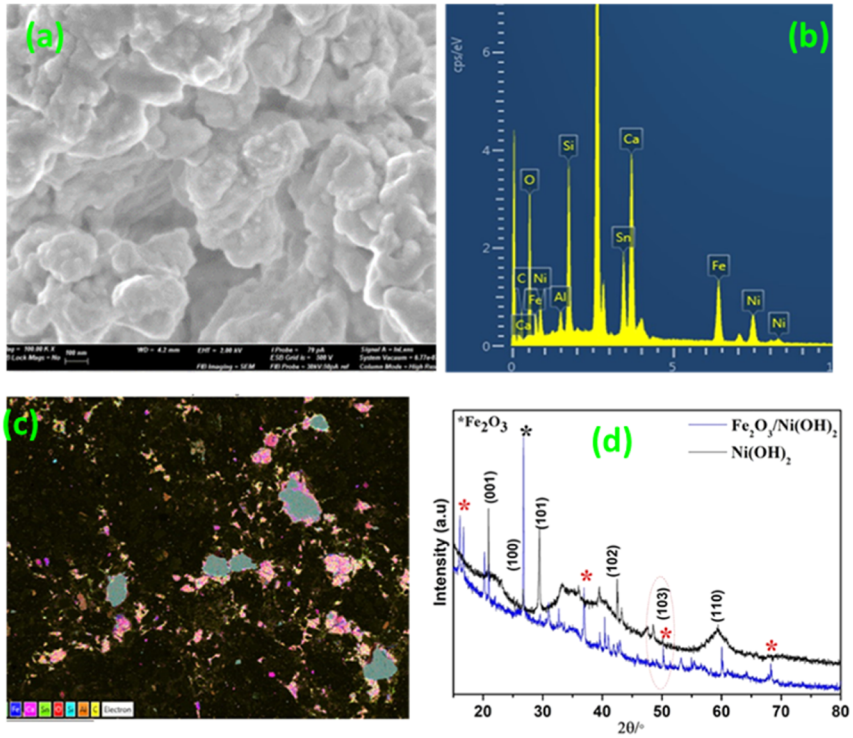

Figure 6. SEM micrograph (a); EDX spectra (b); SEM−EDX overall element map (c); and XRD pattern (d) of $Fe_2O_3/Ni(OH)_2$.

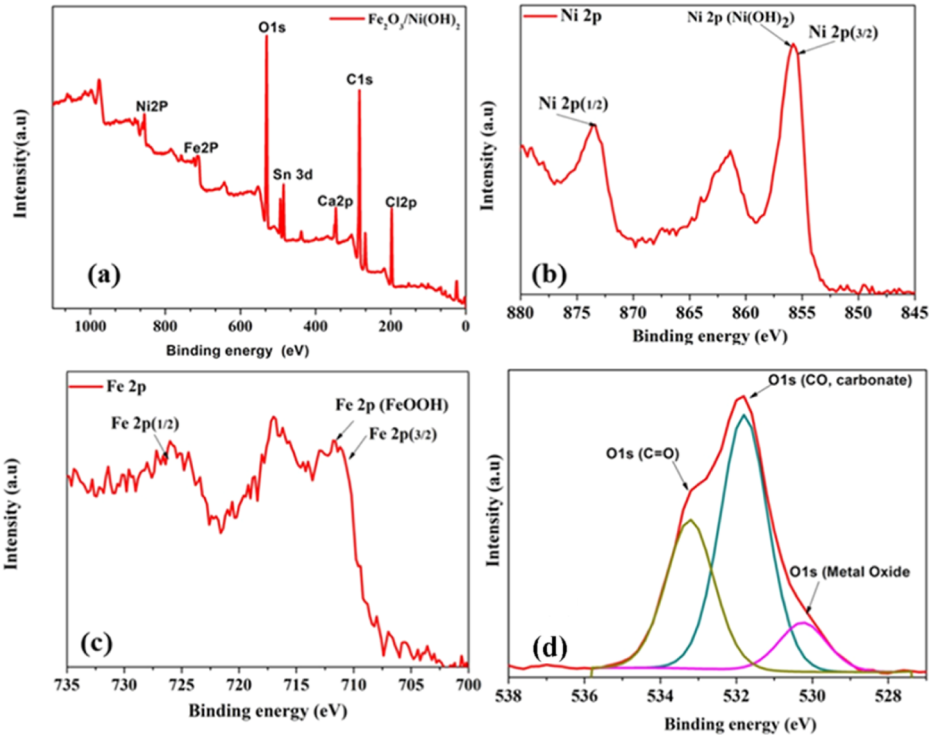

Figure 7. XPS spectra survey of $F_2O_3/Ni(OH)_2$ (a); Fe 2p (b); Fe, Ni 2p (c); and O 1s (d).

peroxide from Merck Group (Pty) Ltd. Throughout the studies, a Milli-Q system Type 1 water (Merck) was used to prepare ultrapure water (18.2 MΩ cm).

4.2. Characterization. In this study, an Agilent 5110 Vertical Dual View (VDV) inductively coupled plasma−optical emission spectrometer (ICP−OES) and Agilent 7800 inductively coupled plasma mass spectrometer (ICP−MS) were used to determine the metal concentration following extraction. The pH of the solutions was measured using an OPR pH meter from Mettler-Toledo Ltd. (Australia). The samples were shaken by hand throughout before the extraction. The precipitated samples were subjected to XRD patterns recording Ultima IV X-ray DI powder diffractometer using Cu Kα radiation operating at 40 kV (diffraction wavelength λ =

https://doi.org/10.1021/acsomega.3c07623
ACS Omega 2024, 9, 5592−5600

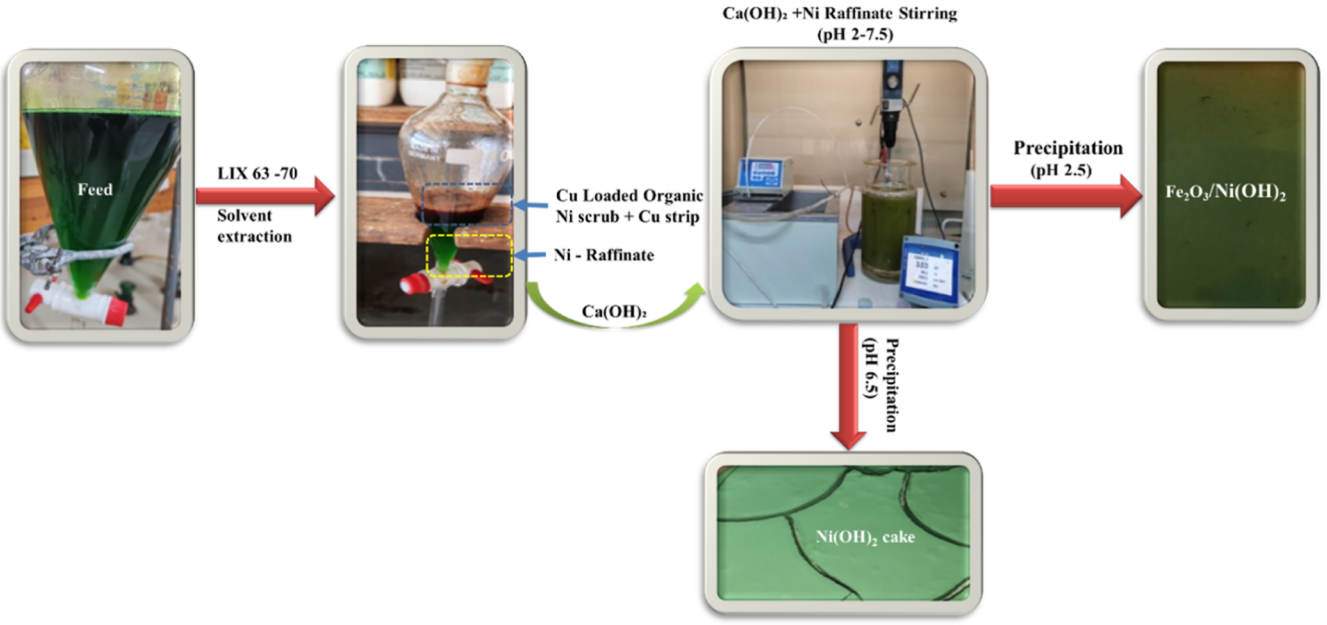

Figure 8. Schematic diagram showing SX and precipitation Ni-case (powder).

0.15406 nm), with a scanning rate of 4°/min throughout the 15 to 90° range to determine the structure of the $Ni(OH)_2$ precipitate. SEM−EDS: Zeiss Cross Beam 540 Morphology Imaging done at 2 kV and 79 pA, working distance 5 mm, InLens detector used. Cross-section imaging was acquired at 20 kV, 5 nA, Backscatter Electron detector was used, and EDS analysis was acquired at 20 kV, 5 nA, Oxford Xmax EDS detector, and Aztec analysis software.

4.3. SX of Cu^{2+}. In this study, all reagents employed met the criteria of reagent grade, except for the commercially sourced extractant. The extraction of Cu was carried out using LIX 63−70, an oxime reagent, with LIX 63−70 serving as an accelerator. Equilibrium studies were meticulously conducted in 125 mL separator funnels, while loading experiments were executed at room temperature with an organic-to-aqueous (O/A) ratio of 1:5. The aqueous phase encompassed a filtrate containing Cu, Ni, and Fe, alongside various other impurities, all encapsulated within a chloride matrix. This comprehensive approach delineates the methodology adopted for the efficient extraction of Cu under specified conditions, shedding light on the crucial components and steps involved in the process.

4.4. Precipitation of Fe^{3+}, Cu^{2+}, and Ni^{2+}. A 2 L jacketed batch reactor equipped with an overhead stirrer was used to ensure effective suspension of the seeding material in the solution, as displayed in Figure 8. Temperature measurements were conducted using a thermometer, while the pH during the reduction process was monitored using a pH meter. The tests were operated at 60 °C and heating was provided by circulating hot water through the jacket of the reactor. The pH of the solution was increased in small increments by using 20% (m/m) $Ca(OH)_2$. The targeted pH points were 2.0, 2.5, 3.0, 3.5, 4.0, 4.5, 5.0, 5.5, 6.0, 6.5, 7.0, and 7.5. After reaching equilibrium at each pH increment, the reactor content was allowed to be stirred for an additional 15 min before a sample was taken and filtered, as well as process parameters, such as pH were recorded. At the end of the test, the slurry was filtered. The volume of filtrate and the mass of residue were recorded. The filter cake was dried at 50 °C overnight in an oven. Solution samples from each pH increment and a sample from the filter cake were analyzed for base metals, HCl, Na, and K.

4.5. Sample Preparation and Analytical Analysis. The elemental concentration in the solutions was analyzed using ICP−OES. The concentration of Na and K was analyzed by AAS. Titration of acid was done by a wet chemistry method. The dissolutions in this study utilized pure HNO_3, and both dissolutions and dilutions were carried out using ultrapure water. Calibration solutions for aqueous ICP−OES in 5% HNO_3 were prepared with materials from high purity standards. ICP−OES measurements were conducted using argon with a purity grade of 99.996%. Sample preparation for ICP−OES analysis involved pipetting a 5 mL sample into a 25 mL volumetric flask, adding 4% nitric acid (HNO_3), 1.25 mL of scandium (Sc) internal standard, and filling to the mark with ultrapure water. The preparation of samples for AAS analysis was diluted 10 times by pipetting 2 and 5 mL samples into a 25 mL volumetric flask with 4% (HNO_3). The acid titration of HCl was done using standardized 1 M of NaOH in an autotitration system with a pH probe and a 1:1 ratio. To cover the entire range of trace and matrix elements in the waste filtrate solution, calibration solutions were made in the following concentration range: from 0.1 to 10,000 ppm. For quality check verification, sample 1, 5, and 11 run was done in duplicates with results within 5% of each other being averaged. The precision of an analytical method is directly influenced by the concentration of the analyte, regardless of the characteristics of the analyte, matrix, or the method employed. This relationship can be determined using the statistical data analysis.

■ ASSOCIATED CONTENT

Supporting Information

The Supporting Information is available free of charge at https://pubs.acs.org/doi/10.1021/acsomega.3c07623.

Utilization of the analytical instruments is essential for evaluating the effectiveness of the SX pretreatment in mitigating Cu loss during precipitation in the presence of Fe, comprehensive analysis of the surface morphol-

https://doi.org/10.1021/acsomega.3c07623
ACS Omega 2024, 9, 5592−5600

ogy, and elemental composition of the sample by EDX and XPS analysis (PDF)

AUTHOR INFORMATION

Corresponding Author

Happy Mothepane Mabowa − *Analytical Chemistry Division, MINTEK, 2155 Randburg, South Africa; School of Chemistry, University of the Witwatersrand, 2050 Johannesburg, South Africa;* orcid.org/0000-0002-8405-4297; Email: happyc@mintek.co.za

Authors

Andile Mkhohlakali − *Analytical Chemistry Division, MINTEK, 2155 Randburg, South Africa*

Sam Mokoena − *Hydrometallurgy Division, MINTEK, 2155 Johannesburg, South Africa*

James Tshilongo − *Analytical Chemistry Division, MINTEK, 2155 Randburg, South Africa; School of Chemistry, University of the Witwatersrand, 2050 Johannesburg, South Africa;* orcid.org/0000-0001-5661-4907

Luke Chimuka − *School of Chemistry, University of the Witwatersrand, 2050 Johannesburg, South Africa*

Complete contact information is available at: https://pubs.acs.org/10.1021/acsomega.3c07623

Notes

The authors declare no competing financial interest.

ACKNOWLEDGMENTS

The authors would like to express sincere gratitude to Mintek for financial support through Science Vote grant number: ASR-00002313 and for permission to publish this work.

REFERENCES

(1) Coman, V.; Robotin, B.; Ilea, P. Nickel recovery/removal from industrial wastes: A review. *Resour., Conserv. Recycl.* **2013**, *73*, 229−238.

(2) El-Naggar, A.; Ahmed, N.; Mosa, A.; Niazi, N. K.; Yousaf, B.; Sharma, A.; Sarkar, B.; Cai, Y.; Chang, S. X. Nickel in soil and water: Sources, biogeochemistry, and remediation using biochar. *J. Hazard. Mater.* **2021**, *419* (May), 126421.

(3) Dermentzis, K. I.; Marmanis, D. I.; Christoforidis, A. K.; Kokkinos, N. C.; Stergiopoulos, D. K., Recovery of metallic nickel from waste sludge produced by electrocoagulation of nickel bearing electroplating effluents *4th International Conference on Sustainable Solid Waste Management*, 2016; pp 23−25.

(4) Krishnan, S.; Zulkapli, N. S.; Kamyab, H.; Taib, S. M.; Din, M. F. B. M.; Majid, Z. A.; Chaiprapat, S.; Kenzo, I.; Ichikawa, Y.; Nasrullah, M.; et al. Current technologies for recovery of metals from industrial wastes: An overview. *Environ. Technol. Innovation* **2021**, *22*, 101525.

(5) Binnemans, K.; Jones, P. T. The Twelve Principles of Circular Hydrometallurgy. *J. Sustain. Metall.* **2023**, *9* (1), 1−25.

(6) Juvonen, R.; Lakomaa, T.; Soikkeli, L. Determination of gold and the platinum group elements in geological samples by ICP-MS after nickel sulphide fire assay: Difficulties encountered with different types of geological samples. *Talanta* **2002**, *58* (3), 595−603.

(7) Strauss, M. L.; Diaz, L. A.; McNally, J.; Klaehn, J.; Lister, T. E. Separation of cobalt, nickel, and manganese in leach solutions of waste lithium-ion batteries using Dowex M4195 ion exchange resin. *Hydrometallurgy* **2021**, *206* (September), 105757.

(8) Ren, Y.; Ran, Y.; Yang, J.; Wei, Y. High Value Conversion Technology of Nickel in Waste Electrolytes of Nitrogen Trifluoride by Electrolysis,. *Separations* **2023**, *10* (9), 477.

(9) Bulut, Y.; Tez, Z. Adsorption studies on ground shells of hazelnut and almond. *J. Hazard. Mater.* **2007**, *149* (1), 35−41.

(10) Phetla, T. P.; Ntuli, F.; Muzenda, E. Reduction crystallization of Ni, Cu, Fe and Co from a mixed metal effluent. *J. Ind. Eng. Chem.* **2012**, *18* (3), 1171−1177.

(11) Taseidifar, M.; Makavipour, F.; Pashley, R. M.; Rahman, A. M. Removal of heavy metal ions from water using ion flotation. *Environ. Technol. Innovation* **2017**, *8*, 182−190.

(12) Keane, M. A. The removal of copper and nickel from aqueous solution using Y zeolite ion exchangers. *Colloids Surf., A* **1998**, *138* (1), 11−20.

(13) Tünay, O.; Kabdaşli, N. I. Hydroxide precipitation of complexed metals. *Water Res.* **1994**, *28* (10), 2117−2124.

(14) Lu, H.; Wang, J.; Yan, B.; Bu, S. Recovery of nickel ions from simulated electroplating rinse water by electrodeionization process. *Water Sci. Technol.* **2010**, *61* (3), 729−735.

(15) Zhang, X.; Zeng, L.; Wang, Y.; Tian, J.; Wang, J.; Sun, W.; Han, H.; Yang, Y. Selective separation of metals from wastewater using sulfide precipitation: A critical review in agents, operational factors and particle aggregation. *J. Environ. Manage.* **2023**, *344* (June), 118462.

(16) Bader, N. Sample preparation for flame atomic absorption spectroscopy : An overview. *Rasayan J. Chem.* **2011**, *4*, 49.

(17) Mahmoud, M. E.; Kenawy, I. M. M.; Hafez, M. A. H.; Lashein, R. R. Removal, preconcentration and determination of trace heavy metal ions in water samples by AAS via chemically modified silica gel N-(1-carboxy-6-hydroxy) benzylidenepropylamine ion exchanger. *Desalination* **2010**, *250* (1), 62−70.

(18) Pham, A. N.; Rose, A. L.; Feitz, A. J.; Waite, T. D. Kinetics of Fe(III) precipitation in aqueous solutions at pH 6.0−9.5 and 25°C. *Geochim. Cosmochim. Acta* **2006**, *70* (3), 640−650.

(19) Younas, M.; Druon-Bocquet, S.; Romero, J.; Sanchez, J. Experimental and Theoretical Investigation of Distribution Equilibria and Kinetics of Copper(II) Extraction with LIX 84 I and TFA. *Sep. Sci. Technol.* **2015**, *50* (10), 1523−1531.

(20) Nozari, I.; Azizi, A. An Investigation into the Extraction Behavior of Copper from Sulfate Leach Liquor Using Acorga M5640 Extractant: Mechanism, Equilibrium, and Thermodynamics. *Min., Metall., Explor.* **2020**, *37* (5), 1673−1680.

(21) Hosseinzadeh, M.; Petersen, J.; Azizi, A. Solvent Extraction Studies of Copper from a Heap Leach Liquor Using Mextral 5640H. *Minerals* **2022**, *12* (10), 1322−1414.

(22) Panigrahi, S.; Parhi, P. K.; Sarangi, K.; Nathsarma, K. C. A study on extraction of copper using LIX 84-I and LIX 622N. *Sep. Purif. Technol.* **2009**, *70* (1), 58−62.

(23) Park, H. W.; Chae, J. S.; Park, S.; Kim, K.; Roh, K. C. Nickel-based layered double hydroxide from guest vanadium oxide anions. *Met. Mater. Int.* **2013**, *19* (4), 887−894.

(24) Qin, Z.; Wang, Y.; Huang, X.; Shen, W.; Yu, J.; Li, J. A Facile Synthesis of Three Dimensional β-Ni(OH)2 Composed of Ultrathin Nanosheets for High Performance Pseudocapacitor. *J. Inorg. Organomet. Polym. Mater.* **2020**, *30* (6), 2089−2097.

(25) Thimmasandra Narayan, R. Effect of Crystallinity of β- and β_{bc}-Nickel Hydroxide Samples on Chemical Cycling. *Indian J. Mater. Sci.* **2015**, *2015*, 1−7.

(26) Mkhohlakali, A. C.; Fuku, X.; Modibedi, R. M.; Khotseng, L. E.; Ray, S. C.; Mathe, M. K. Electrosynthesis and characterization of PdIr using electrochemical atomic layer deposition for ethanol oxidation in alkaline electrolyte. *Appl. Surf. Sci.* **2020**, *502* (October 2019), 144158.

(27) Yu, X.; Zhao, J.; Zheng, L. R.; Tong, Y.; Zhang, M.; Xu, G.; Li, C.; Ma, J.; Shi, G. Hydrogen Evolution Reaction in Alkaline Media: Alpha- or Beta-Nickel Hydroxide on the Surface of Platinum? *ACS Energy Lett.* **2018**, *3* (1), 237−244.

(28) Huotari, J.; Kekkonen, V.; Puustinen, J.; Liimatainen, J.; Lappalainen, J. Pulsed Laser Deposition for Improved Metal-oxide Gas Sensing Layers. *Procedia Eng.* **2016**, *168*, 1066−1069.